CYCLIC FATIGUE BEHAVIOR OF GLASS FIBER REINFORCED EPOXY RESIN AT AMBIENT AND ELEVATED TEMPERATURES

David Kraus[1] and Volker Trappe[2]

[1]Division of Mechanics of Polymers, Bundesanstalt für Materialforschung und -prüfung (BAM), 12200 Berlin, Germany
Email: David.Kraus@bam.de, Web Page: http://www.bam.de
[2]Division of Mechanics of Polymers, Bundesanstalt für Materialforschung und -prüfung (BAM), 12200 Berlin, Germany
Email: Volker.Trappe@bam.de, Web Page: http://www.bam.de

Keywords: composite, fatigue, thermomechanics, residual stresses, temperature

Abstract

The fatigue behavior of ±45° glass fiber reinforced epoxy resin under cyclic mechanical and constant thermal loading is investigated in this study. Tests at three different temperature levels in the range 296 K to 343 K have been performed in order to create S-N curves for each temperature level. The specimen damage is measured in-situ using optical grayscale analysis. The characteristic damage state (CDS) is evaluated for each specimen. It is shown that the point of CDS is suitable as a failure criterion to compare the resulting S-N curves. With micromechanical formulations, the temperature-dependent matrix effort is calculated for each stress-temperature level. In terms of matrix effort, the longest fatigue life is reached at high temperatures, while, in terms of stress, the lowest fatigue life is reached at the highest temperatures.

1. Introduction

In a variety of applications, i.e. aerospace or wind turbine rotor blades, fiber reinforced polymer (FRP) structures are often subjected to quasi-static and cyclic mechanical loading in a wide range of temperature conditions. For the design of these composite structures, a precise knowledge of the material behavior under static and cyclic thermomechanical loading is essential.
The thermomechanical fatigue behavior of the FRP material is affected by the temperature-dependent properties of its constituents. In particular, the properties of the epoxy matrix change substantially at elevated temperatures. In multi-angled laminates, interlaminar residual stresses appear due to the orthotropic thermal expansion behavior of each lamina. Furthermore, residual stresses within a unidirectional layer occur due to thermal expansion, moisture absorption, and shrinkage of the matrix in thermomechanically-loaded FRPs [1]. The temperature dependence of the mechanical properties of the constituents and the composite material, as well as the correlation between damage initiation under quasi-static loading and temperature variation have, been revealed in former studies [2].

In this study, the temperature-dependent fatigue behavior of ±45° glass fiber reinforced polymer is investigated. The composite material combination of Advantex SE1500 glass fibers and RIM 135 epoxy resin is examined. Specimens are subjected to oscillatory uniaxial loads at various testing temperatures in the range 296 K to 343 K.

2. Theory

Structural FRP parts with a ±45° layup are widely used for mainly shear loaded applications, e. g. shells of wind turbine rotor blades or general aviation aircrafts, shear webs of structural beams and for torsion tubes [3].
The inner stress state of each unidirectional ply of a ±45° reinforced specimen that is subjected to a uniaxial tension load in the 0°-direction can be calculated using the classical laminate theory (CLT). Interlaminar residual thermal stresses are considered an external load for each layer in CLT [4]. With micromechanical formulation according to Krimmer, an in-situ stress state of the fibers and the matrix inside each layer can be calculated This includes the intralaminar thermal residual stresses, which are caused by the different coefficients of thermal expansion of the matrix and the fiber material [5]. Likewise, the thermoelastic properties of the fiber and matrix material and the unidirectional layer can be calculated with respect to fiber volume fraction φ and temperature T. This has been shown by Kraus and Trappe to be a reasonable approach for calculating the quasi-static damage onset in thermomechanically-loaded glass fiber reinforced polymer specimens in former studies, using a linear correlation between temperature and the elastic modulus E_M as well as the strength R_M of the resin material. The properties of the fiber material are assumed to be temperature-independent in the examined range [2]. With respect to the external loads σ_E, the in-situ matrix stress σ_M can be calculated by:

$$\{\sigma_M\} = \begin{Bmatrix} \sigma_{M1} \\ \sigma_{M2} \\ \sigma_{M3} \\ \tau_{M23} \\ \tau_{M31} \\ \tau_{M21} \end{Bmatrix} = \begin{Bmatrix} \frac{\sigma_{1E}}{E'_L} E'_{ML} \\ \frac{\sigma_{2E}}{E'_T\left(\frac{\sqrt{2\sqrt{3}\,\frac{\varphi}{\pi}}}{E_{FT}} + \frac{1-\sqrt{2\sqrt{3}\,\frac{\varphi}{\pi}}}{E'_{MT}}\right)} \\ \frac{\sigma_{3E}}{E'_T\left(\frac{\sqrt{2\sqrt{3}\,\frac{\varphi}{\pi}}}{E_{FT}} + \frac{\sqrt{3}-\sqrt{2\sqrt{3}\,\frac{\varphi}{\pi}}}{E'_{MT}}\right)} \\ \frac{\tau_{23E}}{G'_{TT}\left(\frac{\sqrt{2\sqrt{3}\,\frac{\varphi}{\pi}}}{G_{FTT}} + \frac{1-\sqrt{2\sqrt{3}\,\frac{\varphi}{\pi}}}{G'_{MTT}}\right)} \\ \frac{\tau_{31E}}{G'_{LT}\left(\frac{\sqrt{2\sqrt{3}\,\frac{\varphi}{\pi}}}{G_{FLT}} + \frac{\sqrt{3}-\sqrt{2\sqrt{3}\,\frac{\varphi}{\pi}}}{G'_{MLT}}\right)} \\ \frac{\tau_{21E}}{G'_{LT}\left(\frac{\sqrt{2\sqrt{3}\,\frac{\varphi}{\pi}}}{G_{FLT}} + \frac{1-\sqrt{2\sqrt{3}\,\frac{\varphi}{\pi}}}{G'_{MLT}}\right)} \end{Bmatrix} + \begin{Bmatrix} E'_{ML}(\alpha_L - \alpha_M)\Delta T \\ E'_{MT}(\alpha_F - \alpha_T)\Delta T \\ E'_{MT}(\alpha_F - \alpha_T)\Delta T \\ 0 \\ 0 \\ 0 \end{Bmatrix} \quad (1)$$

Here, the indices L and T describe the longitudinal (fiber-parallel) and transversal (fiber-perpendicular) direction of the fiber, matrix, or unidirectional layer. The subscript F describes fiber properties, whereas M stands for matrix properties. E_T and E_L represent the elastic moduli of the unidirectional layer in the transverse and longitudinal direction, respectively. The prime superscript indicates that the strain-blocking effect of the matrix is taken into account [2,5]. The equivalent matrix stress σ_{Me} can be calculated with a strain energy approach according to Beltrami [6] in terms of

$$\sigma_{Me} = \sqrt{\sigma_{M1}^2 + \sigma_{M2}^2 + \sigma_{M3}^3 - 2\nu_M(\sigma_{M1}\sigma_{M2} + \sigma_{M2}\sigma_{M3} + \sigma_{M3}\sigma_{M1}) + 2(1+\nu_M)(\tau_{M21}^2 + \tau_{M31}^2 + \tau_{M23}^2)} \quad (2)$$

It has been shown [2] that matrix damage onset occurs under quasi-static loading when the equivalent matrix stress inside the lamina exceeds the temperature-dependent matrix strength R_M. That means the damage criterion for the matrix is given by

$$\frac{\sigma_{Me}}{R_M} = 1 \tag{3}$$

Thus, a matrix effort can be introduced:

$$e_M = \frac{\sigma_{Me}}{R_M} \tag{4}$$

The damage accumulation process of uniaxially loaded FRPs is well understood. Figure 1 shows the typical damage accumulation process in composites during fatigue life, which can be divided into three stages. In Stage I, the damage initiation starts with fiber-matrix debonding and matrix microcracking. The matrix crack density increases until equilibrium is reached. This point is known as characteristic damage state (CDS). Subsequently, a small linear drop in stiffness and small delaminations lead to a linear rise in damage in Stage II. In Stage III, a growth of delaminations and fiber fracture lead to the mechanical failure of the FRP structure [7–9].

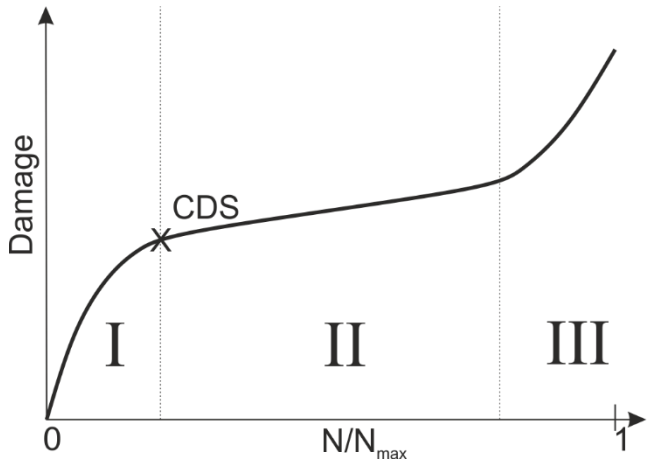

Figure 1: Damage accumulation in fatigue loaded FRPs [7]

The damage inside glass fiber reinforced polymer specimens can be detected using transmitted light, which has been proven to be a suitable method in several studies [10,11]. An in-situ damage value can be obtained by periodically taking photographs of the specimen during fatigue or static tests. Subsequently, the grayscale intensity value of each picture I(N) is processed and a damage parameter D is calculated as follows:

$$D = 1 - \frac{I(N)}{I_0 - [I_{ref,0} - I_{ref}(N)]} \tag{5}$$

Here, I_0 is the grayscale intensity of the undamaged specimen and I_{ref} represents the intensity of a reference area to eliminate small changes in the ambient illumination during the test.

3. Experimental Setup

The fatigue experiments at room temperature have been performed in this study using a ±9 kN servohydraulic tensile/compression test machine with compressed air specimen cooling, while the experiments at elevated temperatures have been performed at a ±40 kN servohydraulic test machine with a climate chamber at a relative humidity of 10%. All tests have been executed in a tension swell range with a load ratio of $R = 0.1$. The testing frequency has been adapted depending on the load level to minimize the temperature rise of the specimens during the test to a maximum of 3 K. The specimen surface temperature has been measured with an infrared thermometer and the temperature in the vicinity of the specimen has been monitored with a thermocouple. Periodically, the test was interrupted and photographs of the specimens were taken at mean stress loading. The specimen layup was $[\pm 45°]_{2S}$ with a specimen size of 140 mm × 20mm × 1.75 mm and a free length of 60 mm. The specimens have been cut out of different plates. For each temperature level, specimens of the same plates have been tested. The mean fiber volume fraction of each whole plate was in the range of $0.52 \leq \varphi \leq 0.56$. The standard deviation in fiber volume fraction for specimens of the same plate was in the range from 0.008 to 0.018.

4. Results and Discussion

The resulting S-N curves with specimen fracture as a failure criterion are plotted in Figure 2. A decrease in fatigue life can be detected for increasing testing temperatures, except for the lowest load level. While the S-N curves at T = 296 K and T = 323 K have a similar slope, the S-N curve for T = 343 K seems to have a different characteristic. This effect matches observations made in previous studies [12].

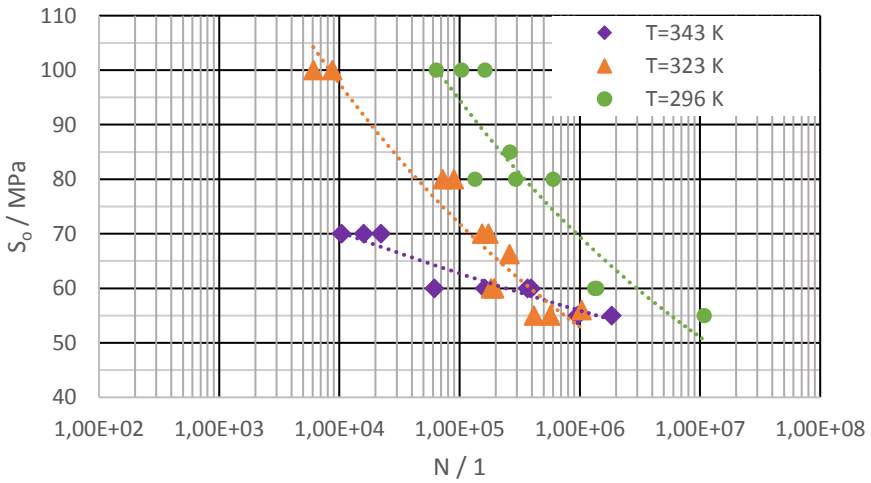

Figure 2: S-N curve for ±45° layup, R = 0.1, failure criterion: specimen fracture

For each fatigue experiment, the point of CDS has been evaluated by means of optical grayscale analysis. This is shown in Figure 3 for a representative specimen at T = 296 K and S_o = 80 MPa. The CDS is defined to be the intersecting point of the actual damage function with a linear fitting curve of the damage in Stage II. This fit is represented by the dashed line in Figure 3.

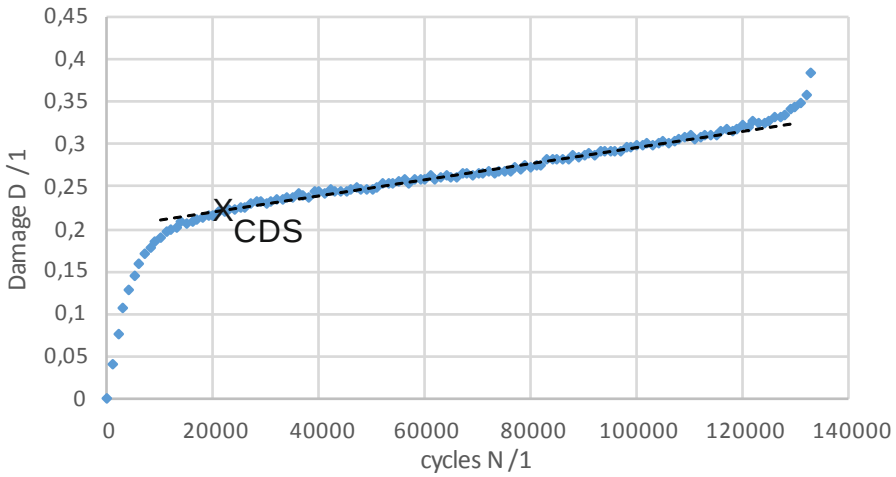

Figure 3: Damage versus load cycles during fatigue for T = 296 K, R = 0.1, S_o = 80 MPa

The CDS can be determined for each specimen and is regarded as a failure criterion for the S-N curve, shown in Figure 4, where N_{CDS} is defined to be the number of cycles, until the CDS is reached. Here, the S-N curves for each temperature level obtain a similar slope. The change in testing temperature now results in a shifting of the load level. In contrast to Figure 2, there is no intersection in the S-N-Curves. Thus, for the specimens, tested at the lowest load level and T = 343 K, a faster damage accumulation compared to T = 323 K happens in Stage I and the CDS is earlier achieved. However, the damage accumulation in Stage II seems to be slower at T = 343 K and the specimen failure occurs after a higher number of load cycles.

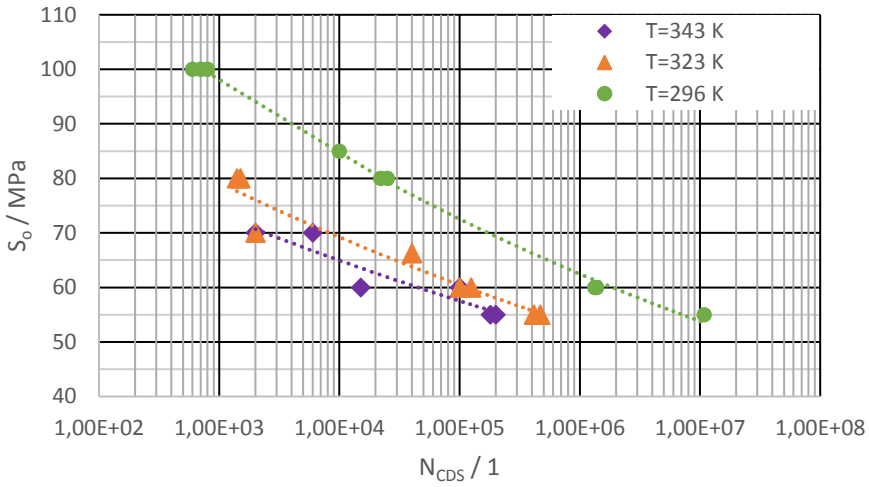

Figure 4: S-N curve for ±45° layup, R = 0.1, failure criterion: CDS

Furthermore, the stress level can be normalized in terms of matrix effort (see Equation 4). Thus, small deviations in fiber volume fraction can be eliminated and the material stress is related to the temperature-dependent tensile matrix strength. This has been computed and experimentally validated using a linear relationship between strength and temperature, and is shown in Table 1 [2].

Table 1. Temperature-dependent matrix strength [2]

Temperature T (K)	Tensile strength $R_M^{(+)}$ (MPa)
296	78.0
323	53.9
343	36.1

The S-N curve with respect to the matrix effort is shown in Figure 5. A normalization of the data into one S-N curve for different testing temperatures is not achieved. A Matrix effort $e_M > 1$ indicates that cracks are forming as of the first load cycle. It becomes apparent, that, in terms of matrix effort, the highest fatigue life is reached at high temperatures. However, in terms of stress, the lowest fatigue life is reached at the highest temperatures. This can be explained by the increasing ductility and decreasing strength of the matrix system at higher temperatures [13].

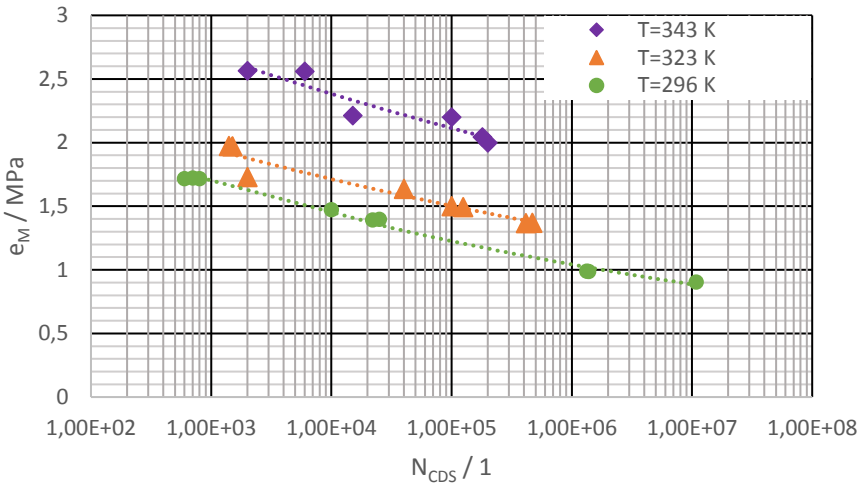

Figure 5: Load cycles vs. matrix effort for ±45° layup, R = 0.1, failure criterion: specimen fracture

5. Conclusion and Outlook

The investigations in this study show a distinct influence of the operating temperature on the fatigue life of ±45° glass fiber reinforced epoxy specimens. Evaluating the CDS leads to comparable results for the different testing temperatures. Furthermore, normalizing the stress level in terms of matrix effort leads to a better understanding of the results. It is beneficial to create a S-N curve for one material where the influence of temperature is normalized. Thus, calculating the fatigue life for other temperature levels would be possible without experimental effort. To reach this goal, a modified micromechanical formulation will be necessary as well as further experimental investigations, i.e. different layups, materials and temperature levels. In particular, the impact of the fiber-matrix interface would have to be taken into account.

Acknowledgments

The work was granted by DFG – Deutsche Forschungsgemeinschaft. The glass fiber materials were provided by European Owens Corning Fiberglas SPRL and the resin was provided by Hexion Inc.

References

[1] Hahn, H. T., 1976, "Residual Stresses in Polymer Matrix Composite Laminates," J. Compos. Mater., **10**(4), pp. 266–278.
[2] Kraus, D., and Trappe, V., 2017, "Impact of Thermal Loads on the Damage Onset of Fiber Reinforced Plastics," *ICCM21 - 21st International Conference on Composite Materials (Proceedings)*, Xi'an, China.
[3] Brøndsted, P., and Nijssen, R. P., 2013, *Advances in Wind Turbine Blade Design and Materials*, Elsevier.
[4] Jeronimidis, G., and Parkyn, A. T., 1988, "Residual Stresses in Carbon Fibre-Thermoplastic Matrix Laminates," J. Compos. Mater., **22**(5), pp. 401–415.
[5] Krimmer, Alexander, Leifheit, Rico, and Bardenhagen, Andreas, 2016, "Assessment of Quasi-Static and Fatigue Performance of Uni-Directionally Fibre Reinforced Polymers on the Basis of Matrix Effort," *6th EASN International Conference on Innovation in European Aeronautics Research*, Porto.
[6] Beltrami, E., 1885, "Sulle condizioni di resistenza dei corpi elastici," Il Nuovo Cimento 1877-1894, **18**(1), pp. 145–155.
[7] Stinchcomb, W. W., 1986, "Nondestructive Evaluation of Damage Accumulation Processes in Composite Laminates," Compos. Sci. Technol., **25**(2), pp. 103–118.
[8] Talreja, R., 1985, "Transverse Cracking and Stiffness Reduction in Composite Laminates," J. Compos. Mater., **19**(4), pp. 355–375.
[9] Talreja, R., and Singh, C. V., 2012, *Damage and Failure of Composite Materials*, Cambridge University Press.
[10] Adden, S., and Horst, P., 2006, "Damage Propagation in Non-Crimp Fabrics under Bi-Axial Static and Fatigue Loading," Compos. Sci. Technol., **66**(5), pp. 626–633.
[11] Talreja, R., 1994, *Damage Mechanics of Composite Materials*, Elsevier.
[12] Harris, B., 2003, *Fatigue in Composites: Science and Technology of the Fatigue Response of Fibre-Reinforced Plastics*, Elsevier.
[13] Fiedler, B., Hobbiebrunken, T., Hojo, M., and Schulte, K., 2005, "Influence of Stress State and Temperature on the Strength of Epoxy Resins," *Proceedings of the 11th International Conference on Fracture (ICF 11)*, Torino, Italy, pp. 2271–2275.